

Liquid-Crystal-Mediated Active Waveguides toward Programmable Integrated Optics

Ting Wei, Peng Chen, Ming-Jie Tang, Guang-Xing Wu, Zhao-Xian Chen, Zhi-Xiong Shen, Shi-Jun Ge, Fei Xu, Wei Hu,* and Yan-Qing Lu*

Optics, playing an ever-important role in life, is developing toward miniaturization and integration. Particularly, the field programming of integrated optics will benefit its functionality and durability, thus is highly pursued. Here, through precisely controlling the space-variant orientations of anisotropic liquid crystals (LCs), various graded-index waveguides are demonstrated in a homogeneous medium. Straight/bending waveguides and ring resonators are fabricated via LC photopatterning. They exhibit pronounced polychromatic light-guiding performance. Thanks to their intrinsic external-stimuli responsiveness, the thermal switchability and polarization tunability are verified. By selectively polymerizing, robust functional components and active connecting waveguides can be realized on the same chip. It provides a practical and universal solution to programmable integrated optics, and extends the applications of microstructured soft matter even in wearable photonics.

Light-based technology is a major economic driver with potential to revolutionize the 21st century as electronics did in the past 20th century. Its rapid advances accelerate the development of science and technology, including information displays, optical communications, computing, and sensing. Similar to the roadmap of electronics, photonics moves toward miniaturization and integration to achieve enhanced functionality and efficient power consumption.^[1,2] One frontier of present electronic technology is field-programmable gate array.^[3] It dynamically connects a series of separate electronic elements on a single chip to perform certain function, thus exhibiting merits of better security and higher durability. These superiorities can also be expected in integrated optics by introducing above strategy. In integrated optics, waveguide is a key enabler for the


connection of various functional components, such as light sources, modulators, and detectors. The waveguide is commonly realized in fine structures of silicon & III-V semiconductors,^[4,5] LiNbO₃,^[6] and polymers,^[7] which guide light via total internal reflection owing to their refractive index differences between surroundings. Programmable functions could be enabled by introducing switchable waveguides to traditional passive integrated optical circuits. The silicon photonics technology is mature,^[4,5] but the high refractive index makes them suffer from significant insertion loss. Although LiNbO₃ presents excellent electro-optical (EO) tunability,^[6] the high driven voltage restricts its EO integration. For polymer optics,^[7] addressable

switching is still a formidable challenge. Therefore, exploiting new materials and techniques for active waveguides remains an urgent task.

The optical anisotropy of liquid crystals (LCs) is determined by the dominant direction of rod-like molecules, i.e., LC director.^[8] Due to its external-stimuli responsiveness, LC becomes a promising candidate for dynamic optics.^[9,10] These years have also witnessed an emergence on the researches of LC involved waveguides. The first strategy is adopting LCs as tunable cladding layers. Due to the polarization dependent light-guiding characteristics, a photoelastic pressure sensor featured by electrical switchability was formed by cladding a low-index LC to an etched single-mode fiber.^[11] Another typical example is filling LCs into the photonic crystal fiber, bringing in a tunable bandgap. The refractive index of LCs can be tuned via both thermal^[12] and electric^[13] field, leading to a switchable wavelength selection. To further improve the integration, the LC hybrid silicon photonics is exploited. The combination of LCs and optical channel waveguide, integrated grating and ring resonator endows the traditional silicon optical circuits with a reconfigurability.^[14–16] Despite of few commercial devices,^[17,18] these heterogeneous configurations suffer from complicated device fabrication and cost inefficiency. On the other hand, the nonlinear spatial solitons in LCs can effectively operate as voltage-controlled steering of self-localized light.^[19–21] However, the rigorous requirement of experimental conditions significantly restricts their practicability. Actually, through precisely controlling the orientation of LCs,^[9] one can arbitrarily manipulate the spatial distribution of refractive index, and thus the propagation of light. The pioneering work about LCs-mediated

T. Wei, Dr. P. Chen, M.-J. Tang, G.-X. Wu, Z.-X. Chen, Z.-X. Shen, Dr. S.-J. Ge, Prof. F. Xu, Prof. W. Hu, Prof. Y.-Q. Lu
National Laboratory of Solid State Microstructures
Key Laboratory of Intelligent Optical Sensing and Manipulation
College of Engineering and Applied Sciences, and Collaborative
Innovation Center of Advanced Microstructures
Nanjing University
Nanjing 210093, China
E-mail: huwei@nju.edu.cn; yqlu@nju.edu.cn

Dr. P. Chen, Dr. S.-J. Ge, Prof. W. Hu
Institute for Smart Liquid Crystals
JITRI
Changshu 215500, China

 The ORCID identification number(s) for the author(s) of this article can be found under <https://doi.org/10.1002/adom.201902033>.

DOI: 10.1002/adom.201902033

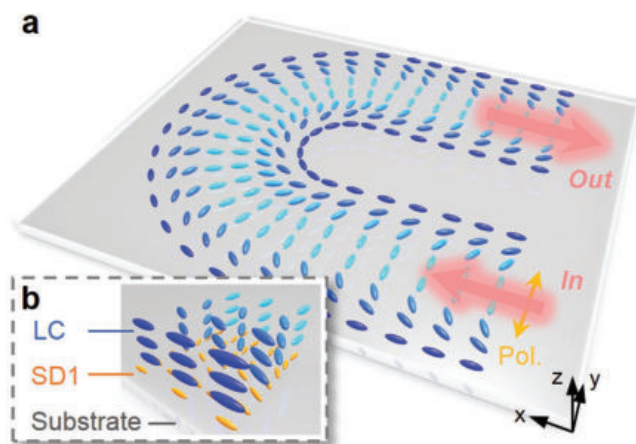


Figure 1. Schematic illustration of the LC waveguide. a) Schematic of the LC director distribution of a bending waveguide with the incident polarization along y axis. Pol., polarization. b) 3D configuration of the LC film on a silica substrate. SD1, photoalignment agent.

step-index straight waveguide^[22] supplies a promising strategy. Unfortunately, it just exploits only a glimpse of opportunities that LCs can offer in this booming topic. Further introducing extra-field stimuli, it may supply a practical platform for programmable integrated optics with a homogeneous medium.

In this work, versatile graded-index waveguides are realized through presetting the in-plane variant LC directors. Straight/bending waveguides and ring resonators are demonstrated via a photopatterning technique, and their performances match well with simulations. The dynamic switch of above waveguides is verified by thermal and polarization control. Achievement of these active waveguides in a homogeneous anisotropic medium makes the programmable integrated optics possible. In addition, photopolymerization further endows the LC circuit with excellent mechanical flexibility.

Thanks to the optical anisotropy, LC can be considered as a uniaxial crystal with optical axis following its local director.

Via controlling the spatial orientation of LC directors, the effective refractive index (n_{eff}) can be rationally designed to support the total internal reflection. **Figure 1** illustrates an LC bending waveguide, whose local director distribution follows the guidance of the photoalignment agent. The directors change gradually along y axis and maintain the same along z axis. Consequently, for x incident light with y polarization, n_{eff} varies from extraordinary (n_e , core) to ordinary (n_o , edge) refractive index continuously, following^[8]

$$n_{\text{eff}} = \frac{n_e n_o}{\sqrt{n_e^2 \sin^2 \alpha + n_o^2 \cos^2 \alpha}} \quad (1)$$

where α represents the angle between the polarization direction and the local director. While for z polarization, n_{eff} keeps n_o everywhere, thus the light guiding effect vanishes. This indicates that such waveguides are polarization sensitive.

We employ the photoalignment technology to imprint the desired space-variant refractive indices into LC director orientations. Photoalignment is very powerful for the ultra-high-resolution and high-quality multidomain alignment of various LCs.^[23–27] A polarization-sensitive sulfonic azo-dye SD1 was used as the photoalignment agent,^[28,29] whose chemical structure is revealed in the inset of **Figure 2a** and absorption spectra in Figure S1b (Supporting Information). Under UV exposure, the molecules of SD1 tend to reorient their absorption oscillators perpendicular to the illuminating polarization. A multistep partly-overlapping exposure was performed with a dynamic photopatterning system.^[9,30] After spin-coated onto the photopatterned substrate, the LCs follow the guidance of SD1 layer and form the designed configuration. The LC precursor, i.e., reactive mesogen mixture can be further photopolymerized into a self-standing flexible film, whose process is vividly presented in Figure 2a. Figure 2b shows the optical setup for the light coupling and observation of the fabricated LC waveguide. Light is efficiently coupled into the waveguide through an optical fiber taper mounted on a 3D moving stage. A polarization controller and a hot stage

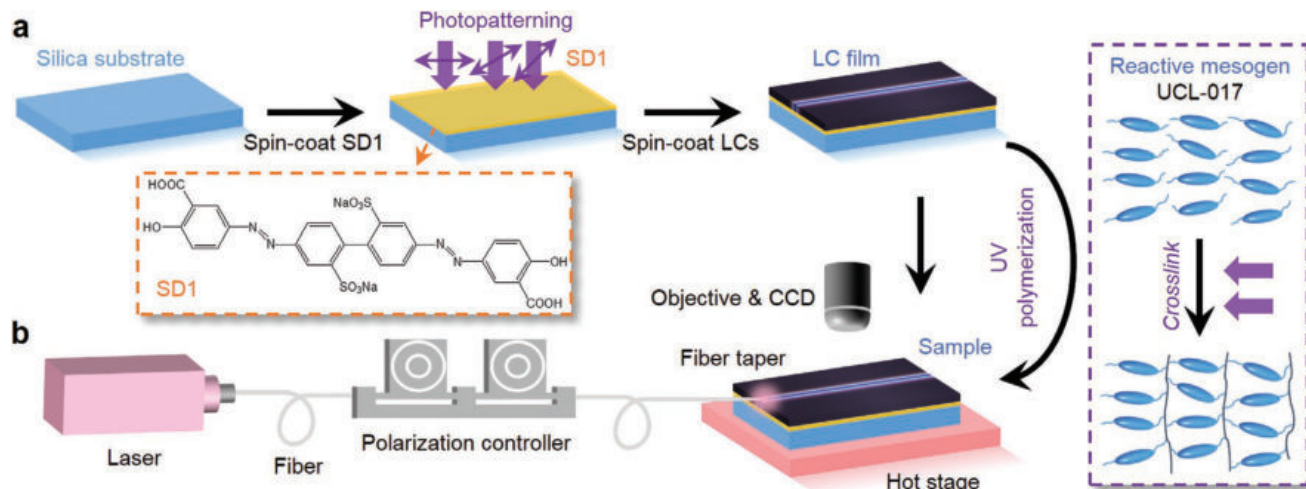


Figure 2. Fabrication process of the LC waveguide and the characterization setup. a) Sequential fabrication procedures of the LC waveguide. Insets: the molecule structure of SD1 (orange); the photopolymerization of UCL-017 (purple). b) The optical setup for light coupling and observation of the LC waveguide. CCD, charge-coupled device.

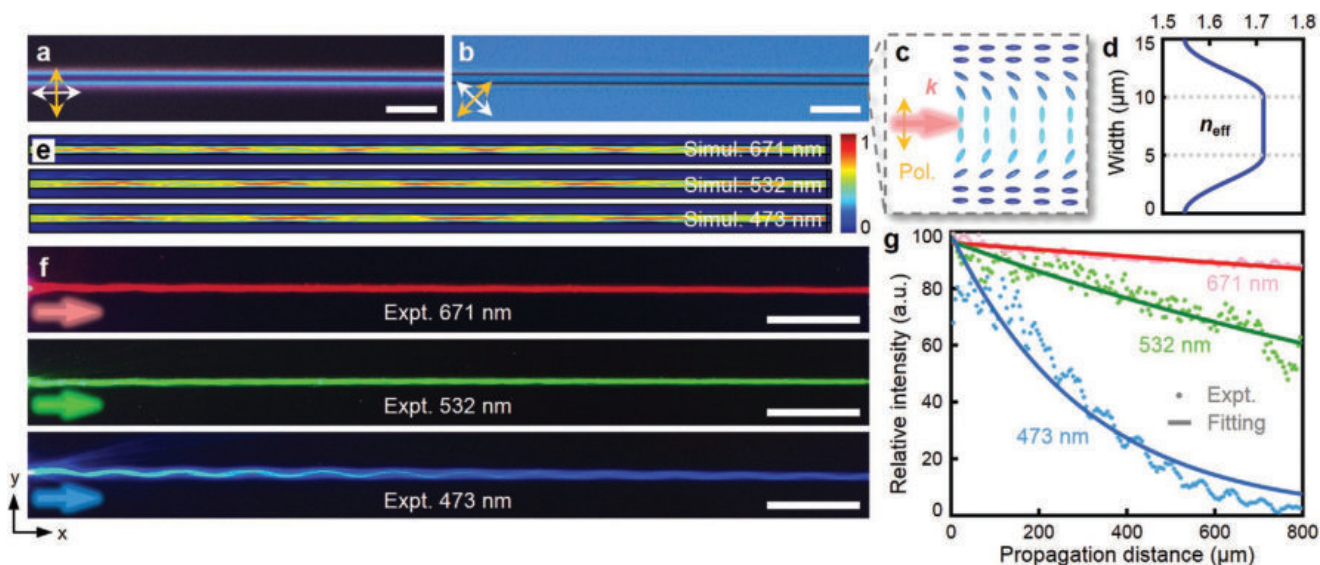


Figure 3. LC straight waveguide. a,b) Micrographs of the straight waveguide under a polarized optical microscope. The polarizer and analyzer are indicated by double-ended arrows, and scale bars indicate 50 μm . c) A top view of the designed LC director distribution. k , the wave vector; Pol., polarization. d) The dependence of n_{eff} on the waveguide width. e) Simulations of the light propagation in the straight waveguide at different wavelengths. Color bar represents the relative intensity of the optical field. f) Experimental images of the straight waveguide at different wavelengths. The arrows indicate the incident direction, and scale bars indicate 100 μm . g) The normalized intensity decay dependent on the propagation distance. The colored dots show the experimental results, while the solid curves show respective fittings.

are used to alternate incident polarization and temperature, respectively.

Figure 3a,b exhibits the micrographs of an LC straight waveguide under crossed polarizers. The continuous change of the brightness is consistent with the continuous varying of the LC director as shown in **Figure 3c**. The width of the core region and each graded-index cladding region are 5 μm , respectively. For γ polarization, the dependency of n_{eff} on the waveguide width is depicted in **Figure 3d**. n_{eff} maintains n_e inside the core and gradually decreases to n_o in the graded-index cladding. Two extra uniform alignment regions (n_o) are preset outside the cladding to eliminate the scattering loss of random nematic domains. Simulations in **Figure 3e** indicate that the polychromatic light is well-confined in the waveguide.

In our tests, the angle and position of the fiber taper are carefully adjusted to reach the largest coupling efficiency, meanwhile, γ polarization is preset to minimize the transmission loss. **Figure 3f** vividly verifies that different color light is well guided and mainly confined within the preset waveguide regions. The normalized intensity variations along with the propagation distance for different wavelengths are depicted in **Figure 3g**. Generally, the light intensity decreases exponentially as $I(x) = I_0 \times e^{-2\beta x}$, where I_0 is the initial intensity, x is the propagation distance, and β is the loss coefficient. Accordingly, exponential fittings are carried out and the calculated propagation losses are 1.68, 2.33, and 11.7 dB mm^{-1} for $\lambda = 671$, 532, and 473 nm, respectively. The propagation loss is mainly attributed to the intrinsic scattering of the LC, which is theoretically proportional to λ^{-4} .^[31] As vividly revealed in **Figure S1** (Supporting Information), for long wavelength range, the experimental results match well with the theoretical tendency. While, a distinct deviation is observed for the blue light, which can be induced by the extra absorption of the SD1 photoalignment

layer. The better performance at longer wavelength may satisfy the requirements of proof-of-principle concept demonstration for integrated optics.

An integrated optical circuit is composed of separate optical elements with distinguished functions. Most of them work on the basis of the manipulation of light propagation, which can be simply considered as certain deformations of a straight waveguide. Herein, we take the bending waveguide and the ring resonator as instances. **Figure 4a** presents the designed director distribution of an LC bending waveguide. In the bending region, the director varies linearly with the azimuthal angle. The outer radius is 200 μm , and the total width of the waveguide is 15 μm with the same structure as the previous straight waveguide. **Figure 4b** exhibits the obtained bending waveguide. A central defect is observed due to the azimuthally variant alignment. **Figure 4c** shows that the light is well guided and propagates along the 180° bending waveguide, consistent with the simulation (**Figure S2**, Supporting Information). The bending waveguide suits for beam deflection, while ring resonator confines light to a small volume by resonant recirculation, and plays a vital role in minimized filter, isolator, and laser.^[32–34] We fabricate an LC ring resonator (**Figure 4e**) via precisely controlling LC directors (**Figure 4d**). It is composed of a straight waveguide and a circular ring with the nearest distance of $\approx 0.5 \mu\text{m}$. **Figure 4f** exhibits that the input green light is efficiently coupled into the ring, and the track of coupling process can be obviously observed. Thanks to the powerful capabilities of the photopatterning technology, more functional waveguides, such as directional coupler and Mach–Zehnder interferometer, can be reasonably expected.

Further exploring the external-field-stimuli responsivity of LCs may make the active optical waveguide possible. For thermotropic LC, raising the temperature above the clearing

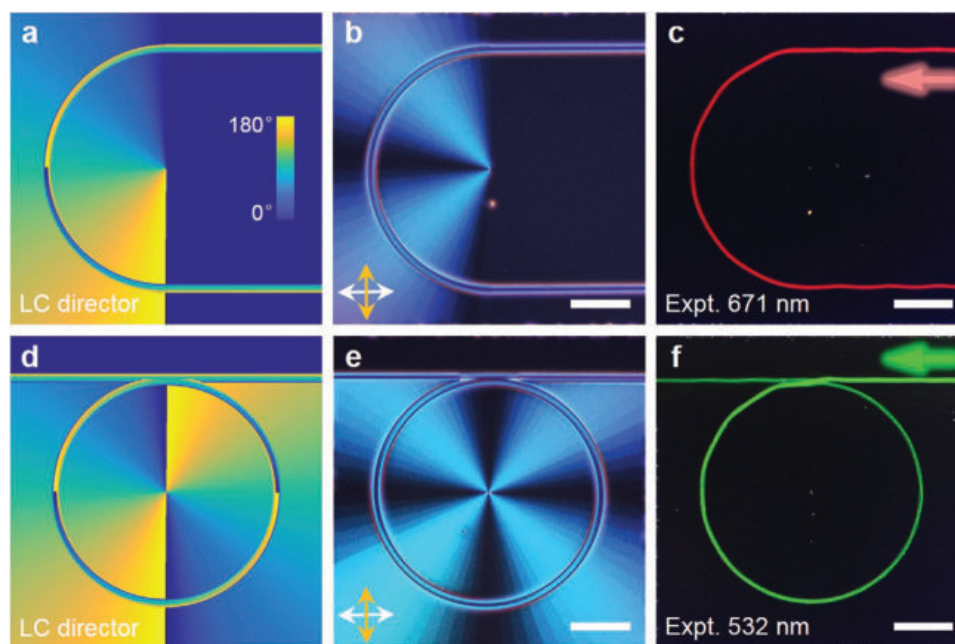


Figure 4. a,d) The designed LC director distributions of the bending waveguide and the ring resonator, respectively. The color variation from blue to yellow indicates the LC director varying from 0° to 180° . b,e) Micrographs under crossed polarizers of the LC bending waveguide and the ring resonator, respectively. The polarizer and analyzer are indicated by double-ended arrows. c,f) Experimental images of the LC bending waveguide and the ring resonator at 671 and 532 nm, respectively. All scale bars indicate $100\ \mu\text{m}$.

point makes the material optical isotropic,^[8] thus the light guiding effect vanishes. The intensity difference between 23 and 58 °C (Figure 5a) verifies the thermal switchability of the straight waveguide. All data are collected in the same waveguide at 671 nm. Thanks to the good thermal stability of SD1, no obvious intensity decay is observed even after tens of thermal-switching cycles, indicating a reliable, reversible, and repeatable control. Corresponding response time is limited to second scale, which is mainly affected by the thermal conductivity of the LC waveguide and the temperature varying speed of the temperature controller. As pervious prediction, this kind of anisotropic waveguide is polarization dependent. Figure 5b shows the dependency of relative intensity on incident polarization direction (θ , defined as the angle between the polarization direction and y axis). The guided light gradually decays and finally breaks down with the polarization rotating from y to z axis (see experimental images in Figure S3, Supporting Information). Experimental results match well with the simulation depicted as the gray solid curve. Besides heat and polarization, such LC waveguide could also be tuned by other stimuli, including electric and optical field.^[35–37]

For programmable integrated optics, functions of components are fixed and only connections among them should be dynamic. To enhance the robustness of these optical components, we further polymerize the LC precursors. Under UV exposure, the LC precursors crosslink and form LC polymer (LCP). After polymerization, the original director distribution is maintained, while the film becomes self-standing and flexible. We transfer the film from the rigid silica to an optically clear adhesive (OCA, 8173D, 3M, USA) film, thus a flexible LC waveguide is obtained. The fabrication process is schematically presented in Figure 5c. A rolled LCP optical circuit with

waveguide structures in different sizes is shown in Figure 5d. Its thermal stability is drastically improved. Here, we take a straight waveguide with a rolled radius of 5 mm as an example. A series of micrographs are captured at different focal planes (Figure 5e). In this case, light still propagates inside the waveguide in spite of an extra rolling loss of $1.55\ \text{dB}\ \text{mm}^{-1}$. Besides repeatable bending, deformations of twisting and stretching are also affordable to such LC waveguides, liberating a full flexibility. By means of patterned UV exposing a same chip, we can selectively polymerize the functional components and leave the connection waveguides active. This makes the programmable integrated optics achievable.

In conclusion, we propose a strategy for graded-index waveguide through precisely controlling the space-variant director distribution of LCs. Straight/bending waveguides and ring resonators are demonstrated with high performance, excellent external field and polarization tunability, and mechanical flexibility. The convenient photopatterning process facilitates their arbitrary design and diverse functionality. Although the proof-of-principle LC waveguides here are multimode, the single-mode one can be rationally anticipated with advanced photopatterning technique of ultrahigh spatial resolution.^[38] This homogeneous medium supplies a simple and practical platform for dynamically connecting separate functional components with active waveguides, making programmable integrated optics available. In addition to traditional rod-like LCs, various 2D LCs^[39–41] can also be introduced, which may bring additional degrees of freedom for manipulation. Especially, the orientation dependent transmittance and reflection would facilitate the attenuation and switch of the LC circuits. By further adopting versatile functional materials,^[42,43] light source and detector could be integrated on the same chip.

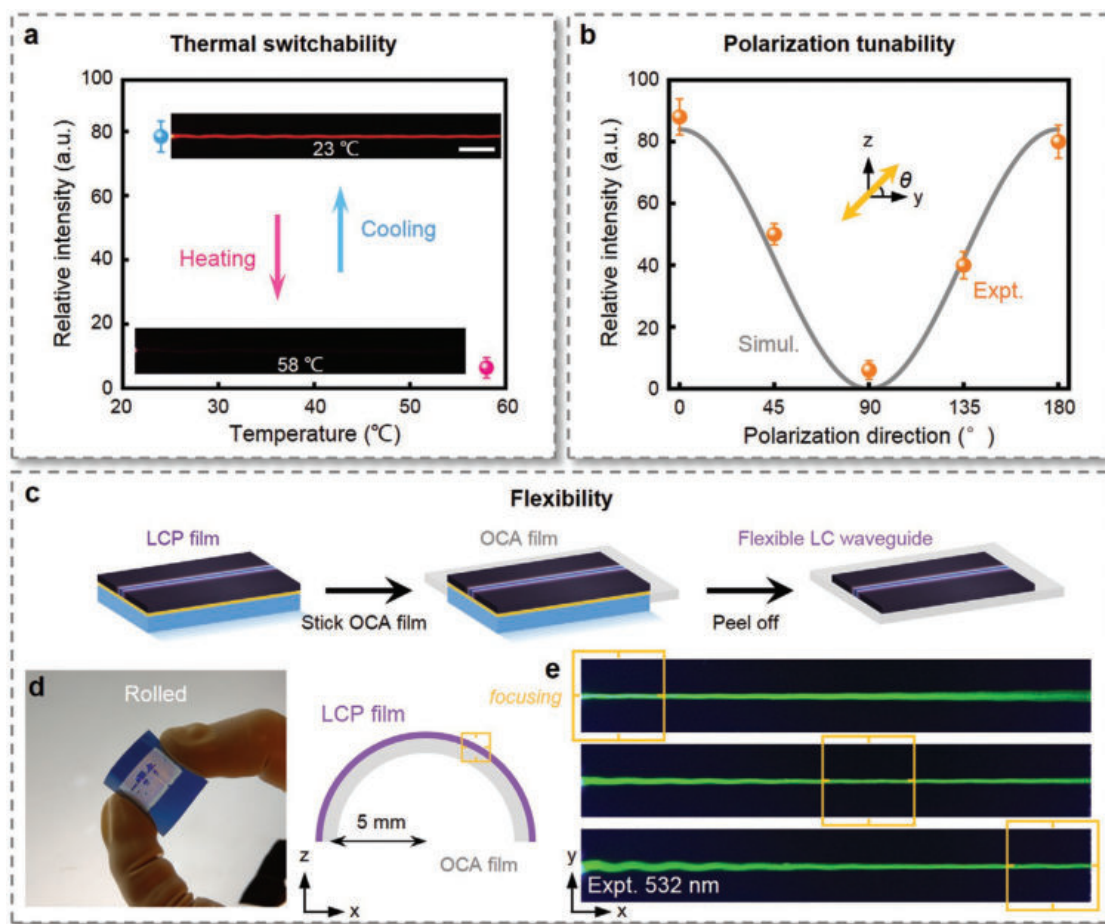


Figure 5. Switchable and flexible LC waveguide. a) Thermal switchability. Insets: images at 23 and 58 °C. Scale bar indicates 100 μm . b) Dependency of relative intensity on incident polarization direction (θ). c) The transfer process of the LCP waveguide onto an OCA film. d) The photograph of a rolled LCP optical circuit and its cross-sectional schematic. e) Experimental images at different focal planes of a rolled waveguide.

This work extends the fundamental understanding of ordered soft matters and is a solid step forward fantastic photonic applications.

Experimental Section

Sample Fabrication: Silica substrates ($1.5 \times 2 \text{ cm}^2$) were ultrasonically bathed, UV-Ozone cleaned, and then spin-coated with the photoalignment agent SD1 (0.3 wt%, DIC, Japan) dissolved in dimethylformamide. The SD1 layer was cured at 100 °C for 10 min to remove the solvent. The sample was then placed at the image plane of a digital microlithography system to accomplish the multistep partly-overlapping exposure process. After the designed orientation recorded, the LC reactive mesogen mixture (50 wt% in methylbenzene, UCL017, DIC, Japan) was spin-coated onto the SD1 layer. The film was heated at 80 °C for residual solvent evaporation and gradually cooled to room temperature. The resultant LC film is $\approx 2 \mu\text{m}$ in thickness. The UV polymerization was performed under a light emitting diode (365 nm, 13 mW cm^{-2}) for 2 min.

Numerical Simulation: COMSOL Multiphysics were used on the basis of the finite-element method. The outer boundaries of the graded-index waveguide were simply treated as the scattering boundary condition and the refractive index of anisotropic LC material was expressed by a matrix. For bending waveguide, the refractive index of bending region was expressed in cylindrical coordinates.

Characterizations: The micrographs of LC waveguides were recorded under the transmissive mode of a polarized optical microscope (Nikon 50i, Japan). The optical fiber taper was drawn from a standard optical single-mode fiber (SMF-28, Corning, USA) using a laser-heated drawing technique. The light guiding behavior of the LC waveguide was recorded through an objective lens in a microscope (Axio Imager A2m, Zeiss, Germany) and captured by a charge-coupled device (CCD) camera (AxioCam MRC 5, Zeiss, Germany).

Supporting Information

Supporting Information is available from the Wiley Online Library or from the author.

Acknowledgements

T.W. and P.C. contributed equally to this work. This work was supported by the National Key Research and Development Program of China (No. 2017YFA0303700), the National Natural Science Foundation of China (NSFC) (No. 61922038), and the Distinguished Young Scholars Fund of Jiangsu Province (No. BK20180004). The authors appreciated Prof. X. S. Jiang for his constructive discussion. W.H. gratefully acknowledges the support of the Tang Scholar program.

Conflict of Interest

The authors declare no conflict of interest.

Keywords

integrated optics, liquid crystals, photoalignment, waveguides

Received: December 3, 2019

Revised: March 2, 2020

Published online:

-
- [1] R. G. Hunsperger, *Integrated Optics*, Springer, Berlin **1995**.
- [2] D. Marpaung, J. P. Yao, J. Capmany, *Nat. Photonics* **2019**, *13*, 80.
- [3] E. Monmasson, L. Idkhajine, M. N. Cirstea, I. Bahri, A. Tisan, M. W. Naouar, *IEEE Trans. Ind. Inf.* **2011**, *7*, 224.
- [4] X. Chen, C. Li, H. K. Tsang, *NPG Asia Mater.* **2011**, *3*, 34.
- [5] W. Bogaerts, L. Chrostowski, *Laser Photonics Rev.* **2018**, *12*, 1700237.
- [6] Y. F. Kong, F. Bo, W. W. Wang, D. H. Zheng, H. D. Liu, G. Q. Zhang, R. Rupp, J. J. Xu, *Adv. Mater.* **2020**, *32*, 1806452.
- [7] H. Ma, A. K. Y. Jen, L. R. Dalton, *Adv. Mater.* **2002**, *14*, 1339.
- [8] I. C. Khoo, S. T. Wu, *Optics and Nonlinear Optics of Liquid Crystals*, World Scientific, Singapore **1993**.
- [9] P. Chen, B. Y. Wei, W. Hu, Y. Q. Lu, *Adv. Mater.* **2019**, 1903665.
- [10] R. S. Zola, H. K. Bisoyi, H. Wang, A. M. Urbas, T. J. Bunning, Q. Li, *Adv. Mater.* **2019**, *31*, 1806172.
- [11] J. Feng, Y. Zhao, S. S. Li, X. W. Lin, F. Xu, Y. Q. Lu, *IEEE Photonics J.* **2010**, *2*, 292.
- [12] T. T. Larsen, A. Bjarklev, D. S. Hermann, J. Broeng, *Opt. Express* **2003**, *11*, 2589.
- [13] F. Du, Y. Q. Lu, S. T. Wu, *Appl. Phys. Lett.* **2004**, *85*, 2181.
- [14] D. Donisi, R. Asquini, A. d'Alessandro, B. Bellini, R. Beccherelli, L. De Sio, C. Umeton, *Mol. Cryst. Liq. Cryst.* **2010**, *516*, 152.
- [15] D. Donisi, B. Bellini, R. Beccherelli, R. Asquini, G. Gilardi, M. Trotta, A. d'Alessandro, *IEEE J. Quantum Electron.* **2010**, *46*, 762.
- [16] W. De Cort, J. Beeckman, T. Claes, K. Neyts, R. Baets, *Opt. Lett.* **2011**, *36*, 3876.
- [17] S. Michael, C. Florenta, Polarization independent liquid crystal waveguides, <https://www.ipms.fraunhofer.de/content/dam/ipms/common/products/AMS/lc-waveguide-e.pdf>, (accessed: February 2020).
- [18] S. R. Davis, S. D. Rommel, S. Johnson, G. Farca, N. Rebolledo, S. Salewyn, M. H. Anderson, presented at *Applied Industrial Optics: Spectroscopy, Imaging and Metrology*, Toronto **2011**.
- [19] M. Peccianti, C. Conti, G. Assanto, A. De Luca, C. Umeton, *Nature* **2004**, *432*, 733.
- [20] N. Karimi, M. Virkki, A. Alberucci, O. Buchnev, M. Kauranen, A. Priimagi, G. Assanto, *Adv. Opt. Mater.* **2017**, *5*, 1700199.
- [21] B. X. Li, V. Borshch, R. L. Xiao, S. Paladugu, T. Turiv, S. V. Shiyonovskii, O. D. Lavrentovich, *Nat. Commun.* **2018**, *9*, 2912.
- [22] M. Rüetschi, P. Rüetschi, J. Fünfschilling, H. J. Güntherodt, *Science* **1994**, *265*, 512.
- [23] M. Schadt, H. Seiberle, A. Schuster, *Nature* **1996**, *381*, 212.
- [24] V. G. Chigrinov, V. M. Kozenkov, H. S. Kwok, *Photoalignment of Liquid Crystalline Materials: Physics and Applications*, Wiley, Chichester, UK **2008**.
- [25] C. H. Peng, T. Turiv, Y. Guo, Q. H. Wei, O. D. Lavrentovich, *Science* **2016**, *354*, 882.
- [26] P. Chen, L. L. Ma, W. Duan, J. Chen, S. J. Ge, Z. H. Zhu, M. J. Tang, R. Xu, W. Gao, T. Li, W. Hu, Y. Q. Lu, *Adv. Mater.* **2018**, *30*, 1705865.
- [27] T. Ouchi, K. Imamura, K. Sunami, H. Yoshida, M. Ozaki, *Phys. Rev. Lett.* **2019**, *123*, 097801.
- [28] H. Akiyama, T. Kawara, H. Takada, H. Takatsu, V. Chigrinov, E. Prudnikova, V. Kozenkov, H. Kwok, *Liq. Cryst.* **2002**, *29*, 1321.
- [29] V. Chigrinov, S. Pikin, A. Verevochnikov, V. Kozenkov, M. Khazimullin, J. Ho, D. D. Huang, H. S. Kwok, *Phys. Rev. E* **2004**, *69*, 061713.
- [30] P. Chen, L. L. Ma, W. Hu, Z. X. Shen, H. K. Bisoyi, S. B. Wu, S. J. Ge, Q. Li, Y. Q. Lu, *Nat. Commun.* **2019**, *10*, 2518.
- [31] S. T. Wu, K. C. Lim, *Appl. Opt.* **1987**, *26*, 1722.
- [32] K. J. Vahala, *Nature* **2003**, *424*, 839.
- [33] S. Y. Hua, J. M. Wen, X. S. Jiang, Q. Hua, L. Jiang, M. Xiao, *Nat. Commun.* **2016**, *7*, 13657.
- [34] X. Y. Xu, W. J. Chen, G. M. Zhao, Y. H. Li, C. Y. Lu, L. Yang, *Light: Sci. Appl.* **2018**, *7*, 62.
- [35] T. J. White, D. J. Broer, *Nat. Mater.* **2015**, *14*, 1087.
- [36] H. K. Bisoyi, Q. Li, *Chem. Rev.* **2016**, *116*, 15089.
- [37] X. L. Pang, J. A. Lv, C. Y. Zhu, L. Qin, Y. L. Yu, *Adv. Mater.* **2019**, *31*, 1904224.
- [38] M. Jiang, Y. B. Guo, H. Yu, Z. Y. Zhou, T. Turiv, O. D. Lavrentovich, *Adv. Mater.* **2019**, *31*, 1808028.
- [39] T. Z. Shen, S. H. Hong, J. K. Song, *Nat. Mater.* **2014**, *13*, 394.
- [40] L. Q. He, J. Ye, M. Shuai, Z. Zhu, X. F. Zhou, Y. N. Wang, Y. Li, Z. H. Su, H. Y. Zhuang, Y. Chen, Z. P. Liu, Z. D. Cheng, J. M. Bao, *Nanoscale* **2015**, *7*, 1616.
- [41] F. Lin, G. Yang, C. Niu, Y. N. Wang, Z. Zhu, H. K. Luo, C. Dai, D. Mayerich, Y. D. Hu, J. Hu, X. F. Zhou, Z. P. Liu, Z. M. Wang, J. M. Bao, *Adv. Funct. Mater.* **2018**, *28*, 1805255.
- [42] H. Coles, S. Morris, *Nat. Photonics* **2010**, *4*, 676.
- [43] M. Schwartz, G. Lenzini, Y. Geng, P. B. Rønne, P. Y. A. Ryan, J. P. F. Lagerwall, *Adv. Mater.* **2018**, *30*, 1707382.